Eur. Radiol. (2001) 11: 325–336

H. W. van Es

MRI of the brachial plexus

Received: 26 June 2000
Accepted: 19 July 2000

H. W. van Es (✉)
Department of Radiology,
St. Antonius Ziekenhuis, Koekoekslaan 1,
3435 CM Nieuwegein, The Netherlands

Abstract Magnetic resonance imaging is the imaging method of first choice for evaluating the anatomy and pathology of the brachial plexus. This review discusses the used imaging techniques, the normal anatomy, and a variety of pathologies that can involve the brachial plexus. The pathology includes primary and secondary tumors (the most frequent secondary tumors being superior sulcus tumor and metastatic breast carcinoma), radiation plexopathy, trauma, thoracic outlet syndrome, neuralgic amyotrophy, chronic inflammatory demyelinating polyneuropathy (CIDP), and multifocal motor neuropathy (MMN).

Key words MRI · Brachial plexus · Tumor · Trauma · CIDP

Introduction

Magnetic resonance imaging is the imaging method of first choice for patients with suspected brachial plexus pathology or for studying the extension of tumors in this region [1, 2, 3, 4, 5, 6]. The brachial plexus is well visualized with MRI due to its excellent inherent contrast differences and the multiplanar capabilities. With ultrasound [7] it is also possible to image the brachial plexus in multiple directions; however, ultrasound is very much operator dependent and it is difficult to image the whole proximal to distal course of the brachial plexus due to the multiple overlying bony structures. Spiral CT [8] can depict the brachial plexus in various directions with the use of multiplanar reconstructions. Magnetic resonance imaging shows more anatomical details and has better contrast differences between the nerves and the surrounding fat compared with CT.

Technique

In 1987 Blair et al. [9] first described the anatomic details of the brachial plexus seen with MRI. The brachial plexus has the same signal intensity as muscle, i.e., low to intermediate on both T1- and T2-weighted images. Turbo spin echo (TSE) imaging and fat suppression can be used [3, 10, 11]. A relatively new technique is MR neurography, which uses a fat-suppressed heavily T2-weighted sequence, e.g., T2-weighted short tau inversion recovery (STIR) imaging. With this sequence nerves can become slightly hyperintense [12]. Magnetic resonance neurography is a very promising technique for the evaluation of peripheral nerve disorders, especially with the use of improved surface coils [13, 14]. Varying imaging strategies have been proposed in the literature. The axial and coronal planes permit left-to-right comparisons. The sagittal plane demonstrates the brachial plexus most consistently because the nerves and the related vessels are seen in cross section. The axial plane is particularly useful for delineating the nerve roots as they exit the foramina, because the imaging plane is then parallel to the orientation of the nerve roots. The coronal plane can show parts of the ventral rami, trunks, divisions, and cords in one plane. However, it is usually impossible to visualize all five ventral rami in one single plane because the upper ventral rami are located anterior to the lower ventral rami due to the cervical lordosis. Several combinations have been recommended: axial and coronal views [1, 15]; axial and sagittal views [16]; sagittal and coronal views with axial slices only scanned on an as-needed basis [17,

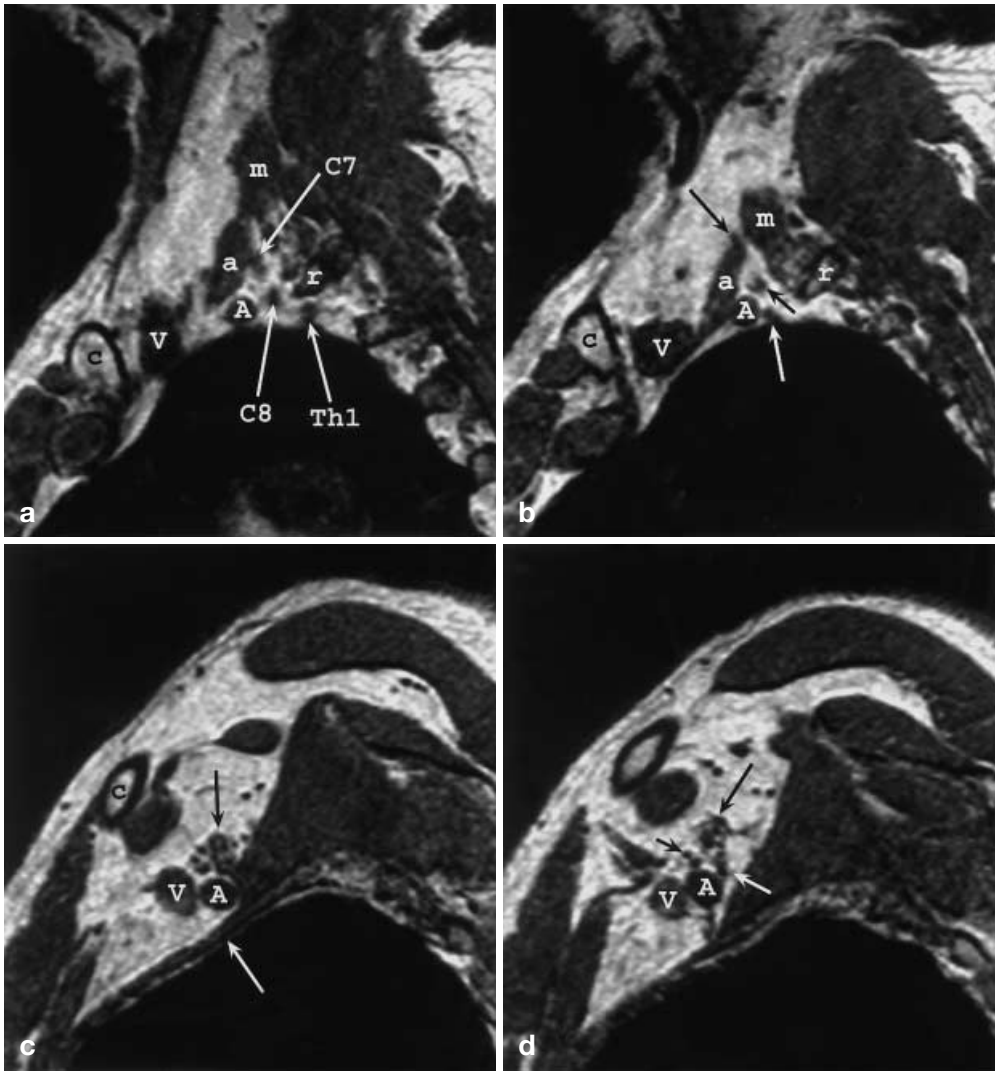

Fig. 1 a–d Normal sagittal anatomy (T1-weighted 3D volume acquisition, slice thickness 1.5 mm). **a** Image at the level of the interscalene triangle with the anterior *(a)* and middle *(m)* scalene muscles. The ventral rami of the roots C7, C8, and Th1 can be discerned. *A* subclavian artery; *V* subclavian vein; *c* clavicle; *r* first rib. **b** Slightly lateral to **a** the three trunks are formed: the upper *(long black arrow)*; middle *(short black arrow)*; and lower *(white arrow)*. **c** The divisions of the brachial plexus *(black arrow)*. *White arrow* points to the first rib. *A* axillary artery; *V* axillary vein. **d** The three cords of the brachial plexus with the lateral cord anterior *(short black arrow)*, the posterior cord superior *(long black arrow)* and the medial cord posterior *(white arrow)* to the axillary artery *(A)*

18]; coronal views with additional axial or sagittal planes [3, 19]; and all planes [5, 11, 20]. The use of oblique coronal images [11] and oblique sagittal images [21] has also been advocated. An alternative for oblique imaging is a T1-weighted three-dimensional (3D) volume acquisition [22] with the availability of thin overlapping slices and multiplanar reconstructions.

Anatomy

The brachial plexus originates from the lower four cervical roots (C5–C8) and the first thoracic root (Th1). The ventral rami of C5, C6, C7, C8, and Th1 form the proximal extent of the brachial plexus and run inferolaterally to enter the interscalene triangle, which is formed by the anterior and middle scalene muscles (Fig. 1 a). The anterior scalene muscle is located anterior and the middle scalene muscle posterior to the ventral rami. The subclavian artery also lies within the interscalene triangle, and the subclavian vein is located between the anterior scalene muscle and the clavicle. The three trunks are formed at the lateral border of the interscalene triangle (Fig. 1 b). The ventral rami of roots C5 and C6 join to become the upper trunk, the ventral ramus of root C7 continues as the middle trunk, and the ventral rami of roots C8 and Th1 unite to become the lower trunk. Just before or at the point where the brachial plexus passes posterior to the clavicle the divisions are formed (Fig. 1 c). Each of the trunks divides into an anterior and posterior division. Lateral to the first rib's outer border, where the subclavian artery and vein become the axillary artery and vein, the three cords are formed (Fig. 1 d). The lateral cord is formed by the anterior divisions from the upper and middle trunks, the medial cord by the anterior division from the lower

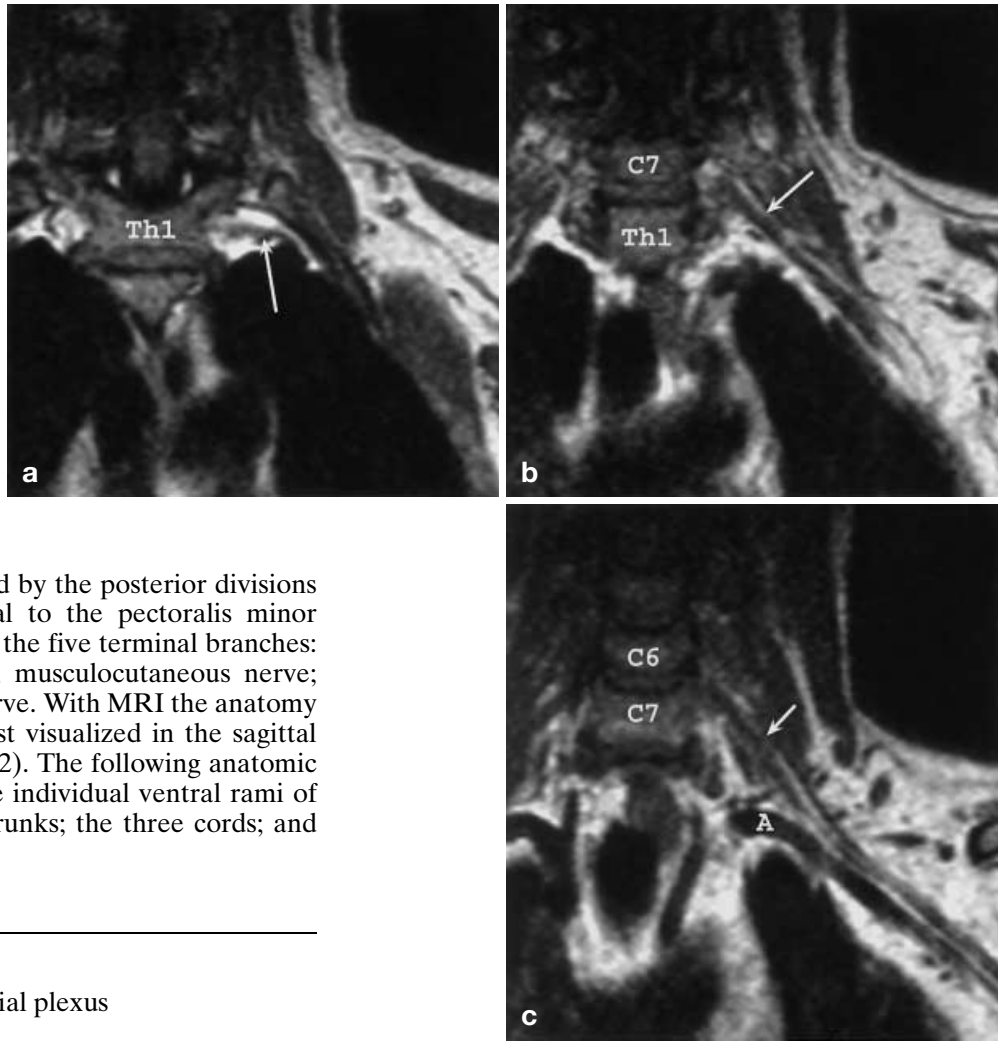

Fig. 2 a–c Normal coronal anatomy (T1-weighted images, slice thickness 3 mm). **a** *Arrow* points to the ventral ramus of the root Th1. **b** Slice more anterior to **a** shows the ventral ramus of the root C8 *(arrow)*. **c** Slice more anterior to **b** shows the ventral ramus of the root C7 *(arrow)*. *A* subclavian artery

trunk, and the posterior cord by the posterior divisions from all trunks. Just lateral to the pectoralis minor muscle the cords divide into the five terminal branches: median nerve; ulnar nerve; musculocutaneous nerve; axillary nerve; and radial nerve. With MRI the anatomy of the brachial plexus is best visualized in the sagittal and coronal planes (Figs. 1, 2). The following anatomic details can be discerned: the individual ventral rami of the nerve roots; the three trunks; the three cords; and the stellate ganglion [22].

Tumors

Primary tumors of the brachial plexus

Primary neurogenic tumors of the brachial plexus are an uncommon but usually well treatable cause of brachial plexopathies [23, 24, 25]. The main primary neurogenic tumors are neurofibromas, schwannomas, and malignant schwannomas. Two large studies, respectively over a 20-year period with 28 tumors [23] and over a 17-year period with 40 tumors [24], found that a neurofibroma is the most common neurogenic tumor of the brachial plexus (50 and 65%, respectively), and that the schwannoma is the second most common neurogenic tumor (18 and 20%, respectively). In both studies 14% of the neural sheath tumors were malignant. A minority (43 and 35%, respectively) of the neurofibromas were associated with von Recklinghausen's disease (neurofibromatosis type I). Neurofibromas can develop in patients with and without von Recklinghausen's disease. A solitary neurofibroma occurs by definition in patients who do not have von Recklinghausen's disease. In patients with von Recklinghausen's disease localized neurofibromas (Fig. 3), which are histologically identical to the solitary neurofibromas, and plexiform neurofibromas occur (Fig. 4) [26]. Neurofibromas have no capsule and infiltrate the nerve fascicles. Because of the diffuse penetration of tumor into the nerve, it is difficult to resect the tumor without permanent damage to the nerve [24]. The schwannoma (Fig. 5) is a benign encapsulated eccentric nerve sheath tumor which arises from Schwann cells and displaces the nerve fascicles instead of infiltrating them. It is usually possible to resect them without sacrificing the nerve or without neurologic damage [24, 25].

Clinical symptoms and signs of primary neurogenic tumors of the brachial plexus can consist of: paresthesias; numbness; sensory and motor deficits, pain; atrophy; and a palpable mass which, when manipulated, can cause radiating paresthesias or pain.

With MRI the detection of primary neurogenic tumors of the brachial plexus has increased [1, 2, 3, 4, 6, 15, 16, 19, 27]. The MRI characteristics of a neurogenic tu-

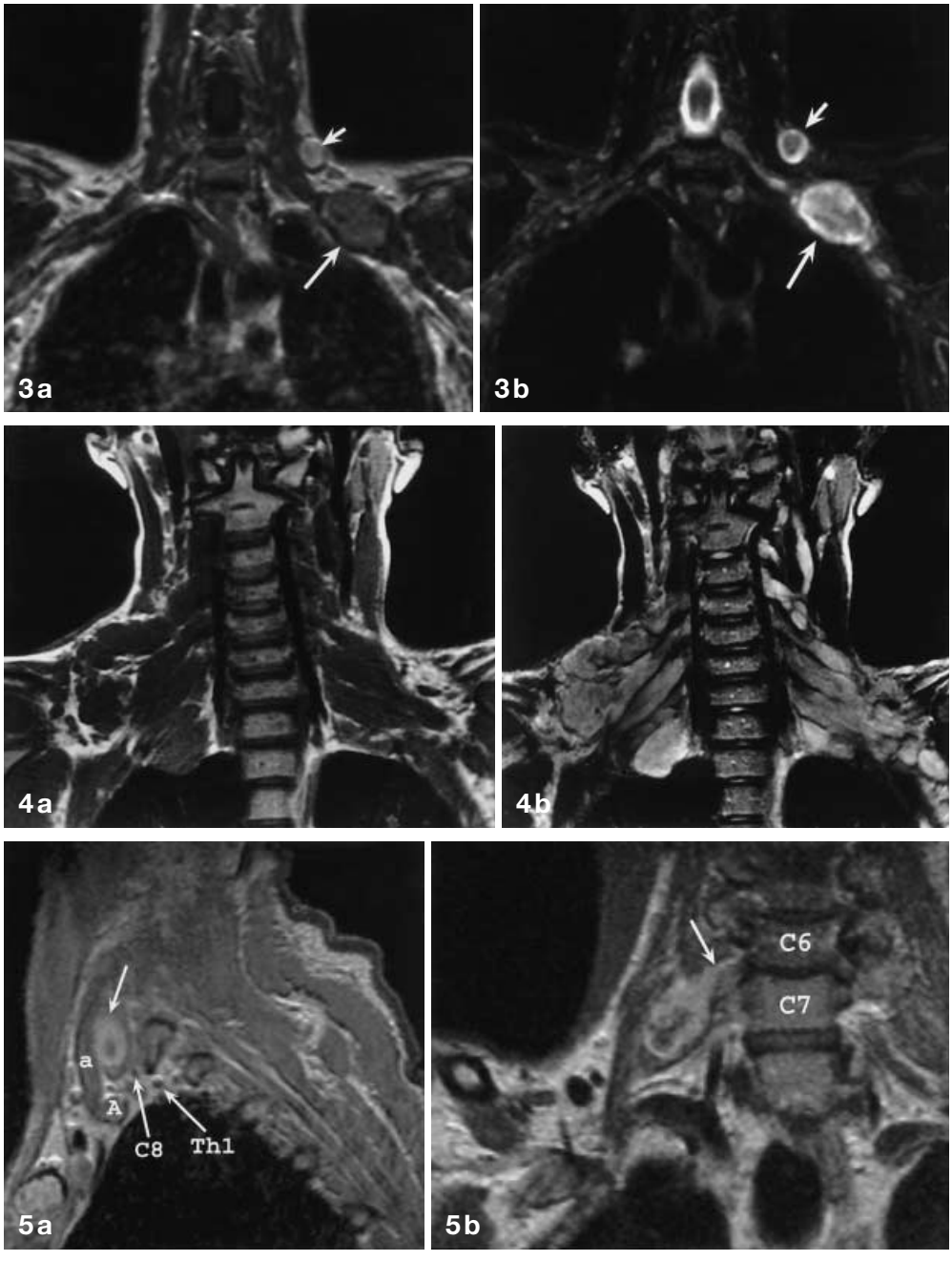

Fig. 3a, b A patient with neurofibromatosis type I and localized neurofibromas. **a** Coronal contrast-enhanced T1-weighted image and **b** a coronal T2-weighted short tau inversion recovery (STIR) image show a large neurofibroma *(long arrow)* of the brachial plexus and a small neurofibroma *(short arrow)* of a subcutaneous nerve

Fig. 4a, b A patient with neurofibromatosis type I and plexiform neurofibromatosis. **a** Coronal T1-weighted image and **b** a coronal fast field echo (FFE) image demonstrate the diffuse enlargement of the brachial plexus on both sides. (Courtesy C. B. L. M. Majoie)

Fig. 5a, b A patient with a schwannoma of C7. **a** Sagittal contrast-enhanced T1-weighted image shows an enhancing tumor *(arrow)* in the interscalene triangle which displaces the anterior scalene muscle *(a)* anteriorly. The ventral rami of the roots C8 and Th1 can be discerned. *A* subclavian artery. **b** Coronal contrast-enhanced T1-weighted image shows the fusiform enhancing tumor, which tapers toward the intervertebral foramen C6–C7 *(arrow)*

mor are: (a) low signal intensity on T1-weighted images, an increased signal intensity on proton-density images, a high signal intensity on T2-weighted images, which can be inhomogeneous, and enhancement after administration of gadolinium; (b) fusiform growth; (c) sharply defined edge; and (d) in many cases the involved nerve can be found entering and leaving the tumor.

With MRI it is not possible to reliably differentiate between a neurofibroma, a schwannoma, and a malignant schwannoma [3, 27, 28].

Superior sulcus tumor (Pancoast's tumor)

Pancoast [29] reported a clinical syndrome associated with a tumor at the apex of the lung. Pancoast's syndrome consists of pain around the shoulder and in the arm in the eighth cervical and first and second thoracic root distribution, Horner's syndrome, muscle atrophy of the hand and radiologic evidence of a shadow at the lung apex always with rib destruction and often with vertebral body involvement. With the superior pulmo-

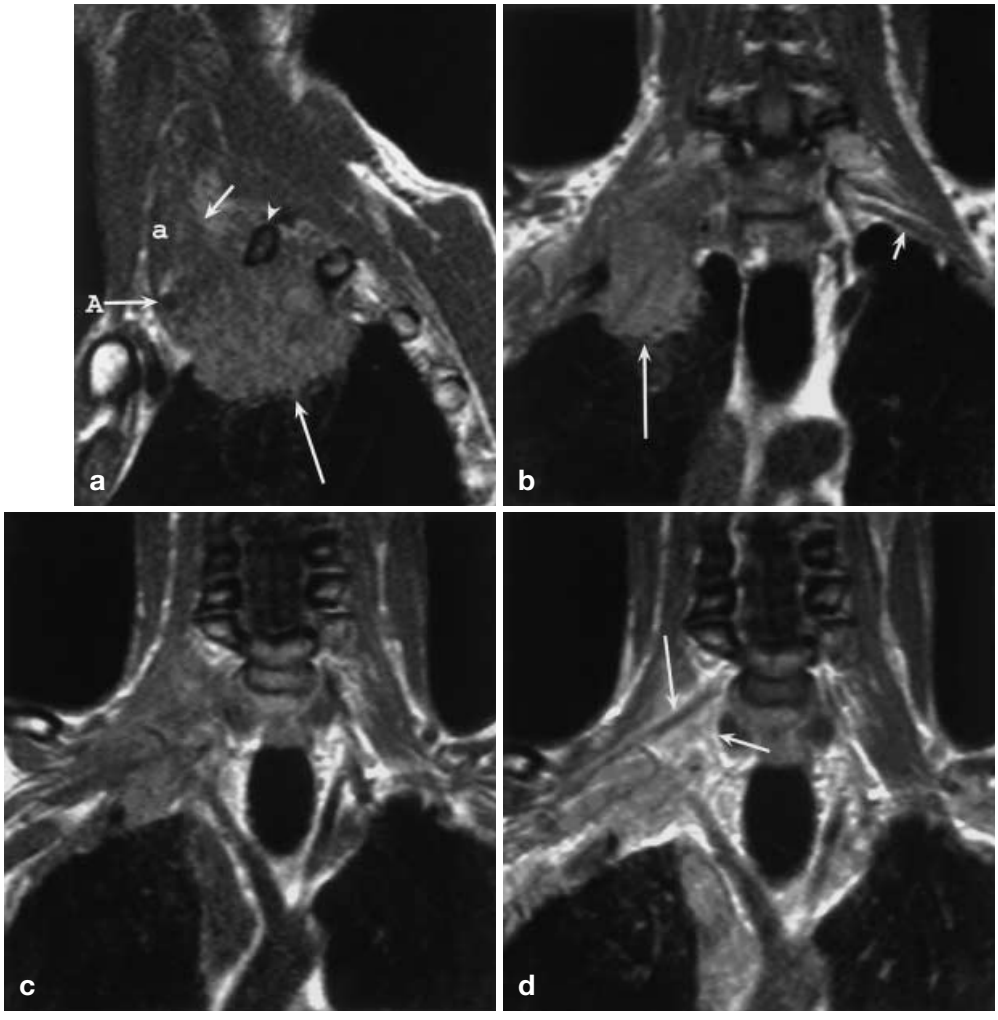

Fig. 6a–d A patient with a superior sulcus tumor (adenocarcinoma) and involvement of the brachial plexus. Preoperatively chemotherapy was given after which the mass in the lung had decreased, and the extension towards the interscalene triangle was unchanged. At surgery, using a combined anterior and posterior approach, it appeared to be possible to remove the tumor totally. The ventral ramus Th1 had to be sacrificed, but the ventral rami of C8 and C7 could be spared. **a** Sagittal T1-weighted image shows a mass in the apex of the lung *(long arrow)* which extends into the interscalene triangle *(short arrow)*. *Arrowhead* points to the first rib with a pathologically decreased signal intensity due to tumor involvement. *A* subclavian artery; *a* anterior scalene muscle. **b** Coronal T1-weighted image permits left-to-right comparison. On the left the ventral ramus of root C8 *(short arrow)* is seen, which has disappeared by the tumor on the right *(long arrow)*. Coronal T1-weighted image **c** without and **d** with gadolinium. With contrast the enhancing tumor *(short arrow)* is seen extending to the ventral ramus of root C7 *(long arrow)*

nary sulcus he presumably meant the anatomical sulcus made by the passage of the subclavian artery in the cupula of the pleura (subclavian artery groove) [30, 31]. As Hepper et al. [30] did not find the anatomic term "superior pulmonary sulcus" in any anatomy book, he suggested the name "thoracic inlet tumor." The term superior sulcus tumor is still widely used despite the fact that this name has been criticized by many authors [32]. Pancoast suggested that the tumor originates from an embryonal rest. The true site of origin, namely the lung, was recognized by Tobias [33]. Hepper et al. [30] demonstrated that these tumors are pathologically identical to other primary tumors of the lung. The histology of superior sulcus tumors can be adenocarcinoma, squamous cell, as well as large cell and small cell carcinomas [31].

According to the TNM classification [34] superior sulcus tumors are by definition at least T3. If there is invasion of the mediastinum or involvement of the heart, great vessels, trachea, esophagus, vertebral body or carina, or presence of malignant pleural effusion the tumor becomes T4 and is considered inoperable in most cases. Any lymph node involvement or distant metastases usually preclude surgery. There are several therapeutic options for the T3N0M0 superior sulcus tumor. Preoperative low-dose radiation therapy followed by surgery, initially reported by Shaw et al. [35], has shown good results: Paulson [31] reported a 5-year survival rate of 34% and a 10-year survival rate of 29%. The purpose of the preoperative radiation therapy is to decrease the extent of disease and to create a pseudocapsule, which increases the resectability. Other therapeutic options are high-dose curative radiation therapy [36, 37], operation and postoperative irradiation [36], and chemotherapy in combination with surgery [36, 37, 38]. There are two major surgical approaches used for the resection of superior sulcus tumors [39, 40]. The classic posterolateral approach [35] is an en bloc resection of the tumor, the involved ribs, and the nerve roots Th1 and C8 if they are involved. A limitation of this

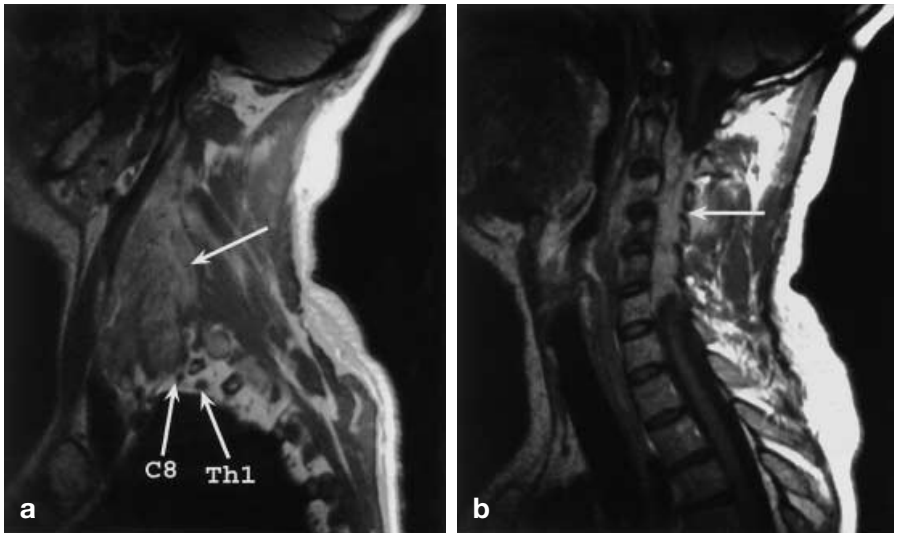

Fig. 7a, b A patient with B-cell non-Hodgkin's lymphoma of the paravertebral lymph nodes with brachial plexus involvement and extradural extension (courtesy B. G. F. Heggelman). **a** Sagittal contrast-enhanced T1-weighted image shows an enhancing tumor *(arrow)* which involves the upper (C5–C7) ventral rami of the nerve roots. The ventral rami of C8 and Th1 are not involved. **b** Sagittal contrast-enhanced T1-weighted image shows an enhancing mass in the spinal canal *(arrow)* consistent with extradural extension of the tumor through the intervertebral foramina

approach is the suboptimal exposure of the structures in the anterior thoracic inlet, such as the brachial plexus and the subclavian vessels. To allow optimal visualization of these vital structures, including the upper part of the brachial plexus, an anterior approach is used [40, 41]. Using the anterior approach a subclavian artery reconstruction can be performed [42], so that surgery in patients with tumor invasion of the subclavian artery is not contraindicated. The anterior approach also permits neurolysis of the brachial plexus without sacrificing the ventral rami of the nerve roots above Th1, even if there is upper brachial plexus involvement. Extensive superior sulcus tumors can be treated with a combination of these two approaches. Vertebral body involvement is not always a contraindication for surgery as a hemivertebrectomy as well as a corpectomy have been described [43, 44]. Absolute contraindications for surgery include distant metastasis, metastasis to mediastinal lymph nodes (N2 disease in the TNM classification [34]), and extensive involvement of the trachea, esophagus and the brachial plexus above the C7 nerve root [40].

The use of MRI has markedly improved the visualization of the superior sulcus tumors (Fig. 6) [4, 45, 46, 47, 48]. The coronal and sagittal planes are especially useful in determining the inferior, superior, posterior, and anterior extent of the tumors. In both planes the relation between the brachial plexus and the tumor can be very well shown. Vertebral body destruction and possible involvement of the nerve roots exiting the foramen are best visualized in the axial plane.

Other tumors and radiation plexopathy

A wide variety of benign and malignant tumors can involve the brachial plexus, including lipoma, aggressive fibromatosis, lymphangioma, sarcoma, head and neck tumors, metastatic disease to lymph nodes or bone, bone tumor, and lymphoma [2, 3, 6, 19, 24].

Lymphoma can involve the brachial plexus in two ways. Firstly, the brachial plexus can be compressed or infiltrated by enlarged lymph nodes. Lymphoma of the paravertebral lymph nodes can extend through the intervertebral foramina to extend to the extradural space (Fig. 7). Secondly, neurolymphomatosis can involve the brachial plexus. Neurolymphomatosis is a rare form of lymphoma, which primarily involves the peripheral nerves [49, 50]. Magnetic resonance imaging shows diffuse thickening and contrast enhancement (Fig. 8) [51].

The most common lymph node metastasis is from breast cancer. Differentiation between brachial plexopathy caused by metastatic disease or radiation therapy is important and can be clinically difficult [52, 53]. Magnetic resonance imaging can be very helpful in the differentiation between tumor and radiation fibrosis [3, 16, 54, 55, 60]. Tumors characteristically have a low signal intensity on T1, a high signal intensity on T2, and enhance with gadolinium; however, the signal intensity characteristics can be variable [60]. Radiation fibrosis usually has a low signal intensity on T1- and T2-weighted images, but can be of high signal intensity on T2-weighted sequences [56, 58, 60]. Radiation fibrosis can also enhance with gadolinium [58]. The most reliable distinction between radiation fibrosis and a tumor is the presence of a mass (Figs. 9, 10) [59, 60].

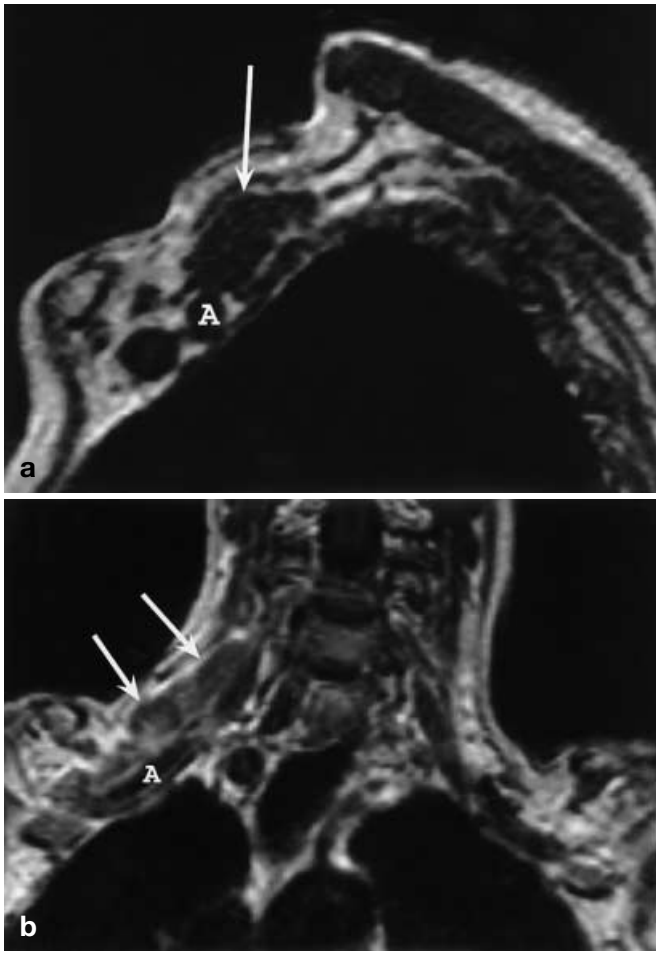

Fig. 8a, b A patient with neurolymphomatosis of the brachial plexus (B-cell non-Hodgkin's lymphoma). **a** Sagittal T1-weighted image at the level of the divisions demonstrates a thickened brachial plexus *(arrow)*. *A* subclavian artery. **b** Coronal contrast-enhanced T1-weighted image shows a slightly enhancing diffusely thickened brachial plexus *(arrows)*

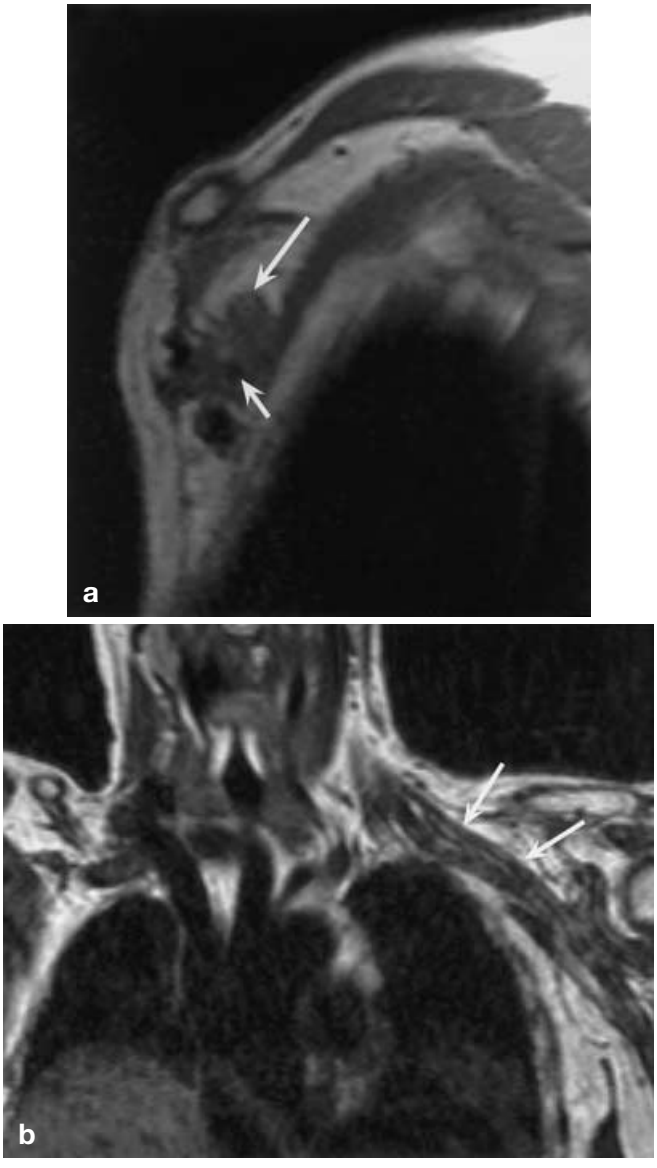

Fig. 9a, b A patient with brachial plexopathy 17 years after a mastectomy. Clinical and MRI follow-up 3 years later showed no change, consistent with radiation fibrosis. **a** Sagittal T1-weighted image shows diffusely thickened cords *(long arrow)* cranially of the axillary artery *(short arrow)*. **b** Coronal T1-weighted image demonstrates a voluminous brachial plexus *(arrows)* without a focal mass lesion

Trauma

Traumatic lesions to the brachial plexus can be divided into supraganglionic (preganglionic) and infraganglionic (postganglionic) lesions. This subdivision has important therapeutic consequences, as a supraganglionic lesion, which is a nerve root avulsion, cannot be repaired directly, whereas the more distal infraganglionic lesions can be restored by local repair.

Nerve root avulsions occur when there is simultaneously traction of the arm and throwing of the head to the opposite side. By far the most common cause in adults is a motorcycle accident. Another important cause is the birth-related brachial palsy. Nerve root avulsions are usually accompanied by traumatic meningoceles; however, traumatic meningoceles can exist without nerve root avulsions and nerve root avulsions can occur without traumatic meningoceles [61]. It is important to determine the site of the lesion, as this has significant prognostic and therapeutic consequences. Reliable imaging of the presence or absence of nerve root avulsions is most important. Computed tomography myelography can depict the nerve roots very well [62]. An important advantage of MRI in the detection of

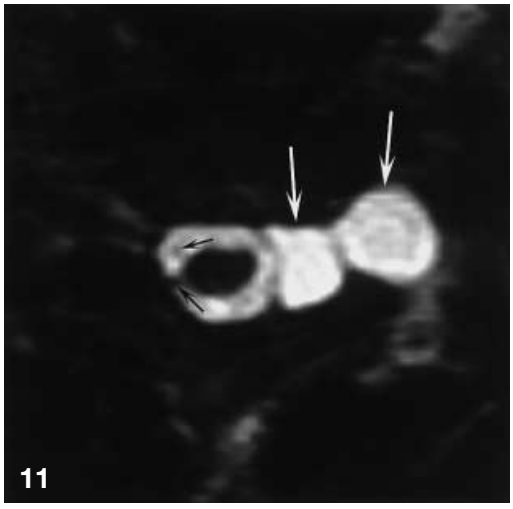

Fig. 10 A patient who developed brachial plexopathy 16 years after a mastectomy. Coronal T1-weighted image shows a focal mass *(white arrow)* involving the brachial plexus *(black arrow)*. Biopsy of the mass revealed metastatic breast cancer. *A* subclavian artery

Fig. 11 A patient with a traumatic meningocele after a motorcycle accident. Axial turbo spin-echo image shows the traumatic meningocele *(white arrows)* on the left. Note the absence of the nerve roots compared with the right *(black arrows)*

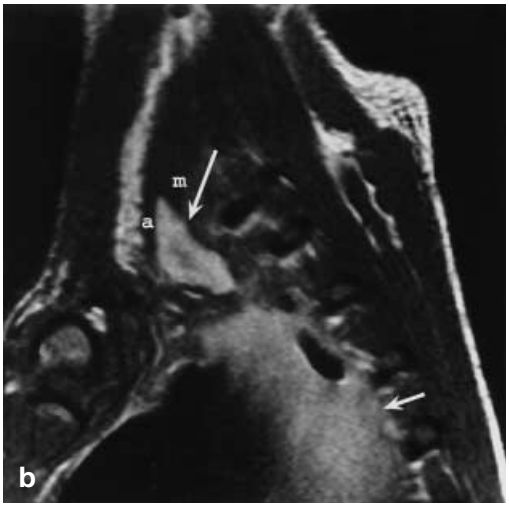

Fig. 12 a, b A patient with a paralyzed arm 5 weeks after a skiing accident. The paralysis spontaneously improved. **a** Sagittal T1-weighted image at the level of the cords demonstrates that the cords *(arrow)* are swollen, consistent with edema. **b** Sagittal T1-weighted image shows a hematoma *(long arrow)* in the interscalene triangle (*a* anterior scalene muscle; *m* middle scalene muscle). *Short arrow* points to a hematothorax

nerve root avulsions is its non-invasiveness: no intradural contrast is necessary. Traumatic meningoceles are fluid collections extending from the neural foramen which follow the signal intensities of the cerebrospinal fluid in all sequences. Magnetic resonance imaging can depict the traumatic meningoceles very well (Fig. 11), even those which do not have a communication with the dural sac, but cannot reliably show all nerve roots [61, 63]. Because, as mentioned previously, traumatic meningoceles occur without nerve root avulsions and nerve roots can avulse without traumatic meningoceles, it is necessary to image the roots themselves and not only the traumatic meningoceles. Computed tomography myelography is considered to be the most reliable investigation for the imaging of the nerve roots [64]. The main advantage of MRI in trauma patients is the visualization of the extraforaminal part of the brachial plexus. Thickening of the brachial plexus (Fig. 12 a) with and without an increased signal intensity on T2-weighted images can be seen, presumably due to, respectively, edema [16, 17] and fibrosis [20, 65]. Magnetic resonance imaging can demonstrate other causes of brachial plexopathy after trauma, such as a hematoma (Fig. 12 b) [1, 3] and a clavicle fracture with brachial plexus compression [1, 3, 66]. The progress of imaging techniques at this time has not been sufficient to preclude diagnostic surgery to define intraoperatively the exact extent of the lesion [67].

Miscellaneous

Thoracic outlet syndrome is a clinical syndrome with controversial therapeutic options. There are three possible sites of compression of the neurovascular bundle: the interscalene triangle; the costoclavicular space be-

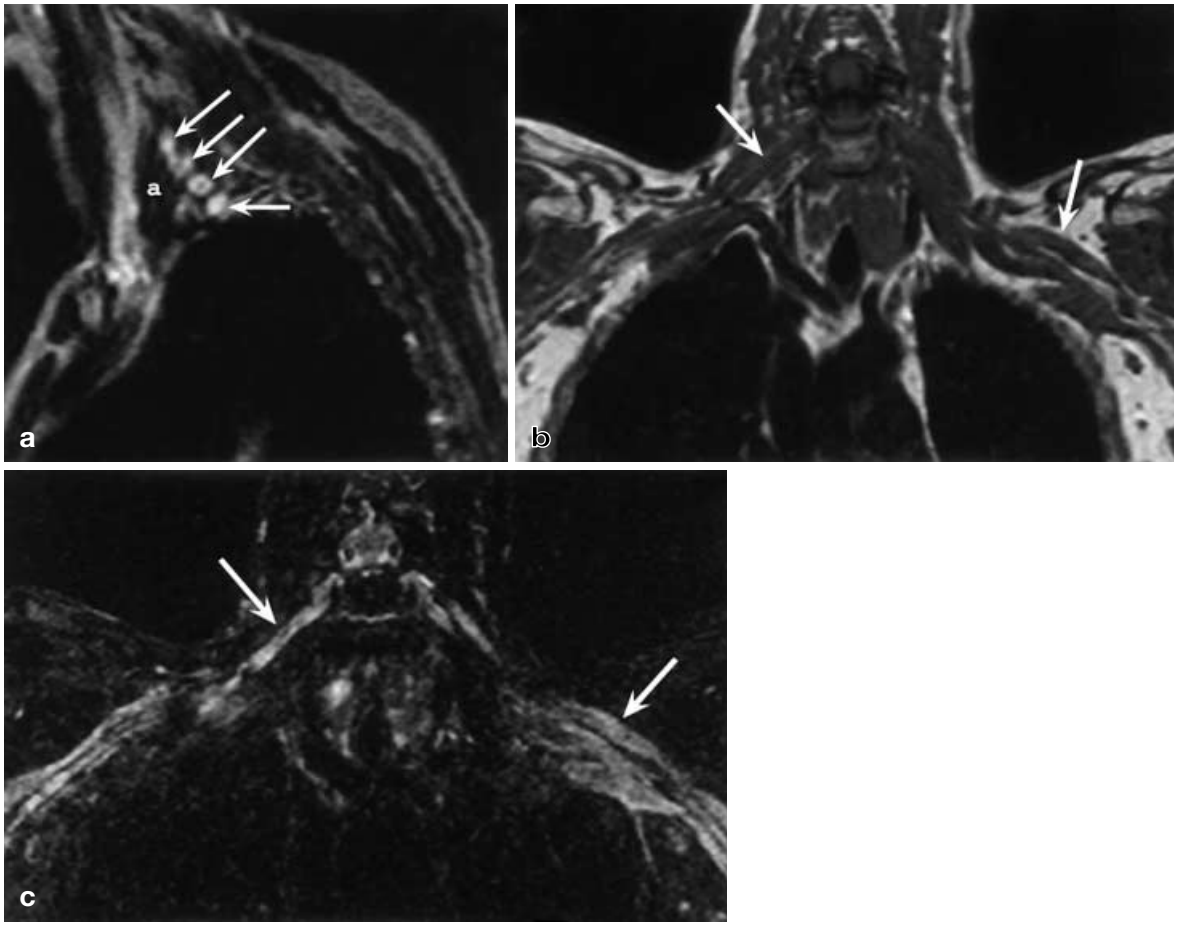

Fig. 13a–c A patient with CIDP. **a** Sagittal T2-weighted image at the level of the interscalene triangle shows an increased signal intensity of the ventral rami of the nerve roots *(arrows)*. *a* anterior scalene muscle. **b** Coronal T1-weighted and **c** T2-weighted STIR image show a slightly thickened brachial plexus on both sides with an increased signal intensity on the STIR image *(arrows)*

tween the clavicle and the first rib; and the subcoracoid tunnel beneath the tendon of the pectoralis minor muscle [8]. The thoracic outlet syndrome is also divided into four subgroups: arterial vascular; venous vascular; true neurogenic; and disputed neurogenic [68]. The true neurogenic thoracic outlet syndrome is a typical clinical syndrome most often found in young women and is associated with an elongated transverse process of C7 or a cervical rib, from which a fibrous band extends to the first rib. The C8 and Th1 ventral rami of the roots or the lower trunk are stretched over this fibrous band [69, 70]. The characteristic clinical picture is that of wasting and weakness of especially the lateral thenar muscles, usually combined with the medial forearm muscles. Other symptoms are pain, paresthesias, and sensory loss along the medial aspect of the arm, forearm, and hand. The therapy is surgical division of this fibrous band [71]. The disputed neurogenic thoracic outlet syndrome includes all disorders in which there is suspected brachial plexus compression without the typical clinical and radiologic findings as seen in the true neurogenic thoracic outlet syndrome. Many symptoms might be present: pain; numbness and paresthesias in the lower trunk distribution; shoulder pain; and back discomfort. Surgical treatment consists of first rib resections or scalenectomies, which can be complicated by serious brachial plexus injuries [70, 72]. Because the clinical picture is unclear, and there are no reliable diagnostic tests, this type is overdiagnosed and overtreated [73]. Imaging can be helpful in making the distinction between the different types of thoracic outlet syndrome. Conventional radiographs show bony abnormalities, which include cervical ribs, elongated transverse processes of C7, and exostoses or old fractures of the first rib and clavicle. Conventional angiography is useful in detecting the major arterial vascular thoracic outlet syndrome, but might be replaced by MR angiography [74, 75]. Spiral CT might be useful in determining the site of vascular obstruction [8]. The value of MRI in diagnosing the neurogenic thoracic outlet syndromes is still uncertain.

With MRI distortion of the brachial plexus can be seen [22]. One article described the MRI findings of a fibrous band, which was called an MRI band [76]. A sensitivity of 79 % and a specificity of 87.5 % were found when the distortion of the brachial plexus on MRI was correlated with the clinical symptoms; however, in the same study an MRI band was also found in three asymptomatic volunteers, which was associated with brachial plexus distortion in one, so that the value of these findings remains unclear. These good results have been criticized by Cherington et al. [77] who disagreed with the MRI abnormalities.

Neuralgic amyotrophy (also known as acute brachial neuropathy, brachial plexus neuropathy, brachial neuritis, Parsonage-Turner syndrome and shoulder girdle syndrome) is a syndrome characterized by acute onset of pain, followed by weakness and atrophy of the shoulder girdle muscles [78, 79]. The prognosis is good: in a series of 99 cases full recovery was seen in over 90 % by 4 years [79]. The etiology of this disorder is not known, but some antecedent events, such as viral infections and immunizations, often herald the onset of neuralgic amyotrophy. An inflammatory-immune pathogenesis has been suggested [80]. With imaging an increased signal intensity on T2-weighted images has been described [3, 5]; however, in another study no abnormalities were detected and MRI served to exclude other structural abnormalities [1]. Other abnormalities found with MRI include atrophy and high signal intensity of the shoulder muscles [81, 82].

Chronic inflammatory demyelinating polyneuropathy (CIDP) and multifocal motor neuropathy (MMN) can affect the brachial plexus. Chronic inflammatory demyelinating polyneuropathy is a sensorimotor neuropathy with symmetric weakness and sensory loss in both arms and legs. Multifocal motor neuropathy presents as an asymmetric weakness without sensory loss. Both CIDP and MMN are probably immune-mediated neuropathies which can respond to high-dose intravenous immunoglobulins [83, 84]. Biopsies of patients with CIDP shows demyelination, remyelination, and inflammation [85]. Magnetic resonance imaging can show hypertrophy and an increased signal intensity on T2-weighted images of the brachial plexus (Fig. 13) [86, 87, 88].

References

1. Bilbey JH, Lamond RG, Mattrey RF (1994) MR imaging of disorders of the brachial plexus. J Magn Reson Imaging 4: 13–18
2. Mukherji SK, Castillo M, Wagle AG (1996) The brachial plexus. Semin Ultrasound CT MR 17: 519–538
3. Posniak HV, Olson MC, Dudiak CM, Wisniewski R, O'Malley CO (1993) MR imaging of the brachial plexus. AJR 161: 373–379
4. Reede DL (1993) Magnetic resonance imaging of the brachial plexus. MRI Clin North Am 1: 185–195
5. Sherrier RH, Sostman HD (1993) Magnetic resonance imaging of the brachial plexus. J Thorac Imaging 8: 27–33
6. Van Es HW (1997) MR imaging of the brachial plexus. Thesis, State University Utrecht, The Netherlands (www.library.uu.nl/ ~ proefsch/01825445/inhoud.htm)
7. Sheppard DG, Iyer RB, Fenstermacher MJ (1998) Brachial plexus: demonstration at US. Radiology 208: 402–406
8. Remy-Jardin M, Doyen J, Remy J, Artaud D, Fribourg M, Duhamel A (1997) Functional anatomy of the thoracic outlet: evaluation with spiral CT. Radiology 205: 843–851
9. Blair DN, Rapoport S, Sostman HD, Blair OC (1987) Normal brachial plexus: MR imaging. Radiology 165: 763–767
10. Posniak HV, Olson MC (1995) Questions and answers. AJR 165: 224–225
11. Panasci DJ, Holliday RA, Shpizner B (1995) Advanced imaging techniques of the brachial plexus. Hand Clinics 11: 545–553
12. Maravilla KR, Aagaard BDL, Kliot M (1998) MR neurography. MR imaging of peripheral nerves. MRI Clin North Am 6: 179–194
13. Hayes CE, Tsuruda JS, Mathis CM, Maravilla KR, Kliot M, Filler AG (1997) Brachial plexus: MR imaging with a dedicated phased array of surface coils. Radiology 203: 286–289
14. Maravilla KR, Bowen BC (1998) Imaging of the peripheral nervous system: evaluation of peripheral neuropathy and plexopathy. AJNR 19: 1011–1023
15. Castagno AA, Shuman WP (1987) MR imaging in clinically suspected brachial plexus tumor. AJR 149: 1219–1222
16. Rapoport S, Blair DN, McCarthy SM, Desser TS, Hammers LW, Sostman HD (1988) Brachial plexus: correlation of MR imaging with CT and pathologic findings. Radiology 167: 161–165
17. Kneeland JB, Kellman GM, Middleton WD, Cates JD, Jesmanowicz A, Froncisz W, Hyde JS (1987) Diagnosis of diseases of the supraclavicular region by use of MR imaging. AJR 148: 1149–1151
18. Van Es HW, Witkamp TD, Feldberg MAM (1995) MRI of the brachial plexus and its region: anatomy and pathology. Eur Radiol 5: 145–151
19. De Verdier HJ, Colletti PM, Terk MR (1993) MRI of the brachial plexus: a review of 51 cases. Comput Med Imaging Graph 17: 45–50
20. Gupta RK, Mehta VS, Banerji AK, Jain RK (1989) MR evaluation of brachial plexus injuries. Neuroradiology 31: 377–381
21. Obuchowski AM, Ortiz AO (2000) MR imaging of the thoracic inlet. MRI Clin North Am 8: 183–203
22. Van Es HW, Witkamp TD, Ramos LMP, Feldberg MAM, Nowicki BH, Haughton VM (1996) MR imaging of the brachial plexus using a T1-weighted three-dimensional volume acquisition. Int J Neuroradiol 2: 264–273
23. Dart LHJ, MacCarty CS, Love JG, Dockerty MB (1970) Neoplasms of the brachial plexus. Minn Med 53: 959–964
24. Lusk MD, Kline DG, Garcia CA (1987) Tumors of the brachial plexus. Neurosurgery 21: 439–453
25. Sell PJ, Semple JC (1987) Primary nerve tumours of the brachial plexus. Br J Surg 74: 73–74
26. Enzinger FM, Weiss SW (1988) Benign tumors of peripheral nerves. In: Soft tissue tumors. Mosby, St. Louis, pp 719–780

27. Stull MA, Moser RPJ, Kransdorf MJ, Bogumill GP, Nelson MC (1991) Magnetic resonance appearance of peripheral nerve sheath tumors. Skeletal Radiol 20: 9–14
28. Suh J, Abenoza P, Galloway HR, Everson LI, Griffiths HJ (1992) Peripheral (extracranial) nerve tumors: correlation of MR imaging and histologic findings. Radiology 183: 341–346
29. Pancoast HK (1932) Superior pulmonary sulcus tumor: tumor characterized by pain, Horner's syndrome, destruction of bone and atrophy of hand muscles. J Am Med Assoc 99: 1391–1396
30. Hepper NGG, Herskovic T, Witten DM, Mulder DW, Woolner LB (1966) Thoracic inlet tumors. Ann Intern Med 64: 979–989
31. Paulson DL (1975) Carcinomas in the superior pulmonary sulcus. J Thorac Cardiovasc Surg 70: 1095–1104
32. Teixeira JP (1983) Concerning the Pancoast tumor: What is the superior pulmonary sulcus? Ann Thorac Surg 35: 577–578
33. Tobias JW (1932) Syndrome apico-costo-vertebral doloroso por tumor, apexiano: su valor diagnostico en el cancer primitivo pulmonar. Rev Med Latin Am 17: 1522–1666
34. Mountain CF (1997) Revisions in the International System for Staging Lung Cancer. Chest 111: 1710–1717
35. Shaw RR, Paulson DL, Kee JLJ (1961) Treatment of the superior sulcus tumor by irradiation followed by resection. Ann Surg 154: 29–40
36. Attar S, Krasna MJ, Sonett JR, Hankins JR, Slawson RG, Suter CM, McLaughlin JS (1998) Superior sulcus (Pancoast) tumor: experience with 105 patients. Ann Thorac Surg 66: 193–198
37. Detterbeck FC (1997) Pancoast (superior sulcus) tumors. Ann Thorac Surg 63: 1810–1818
38. Arcasoy SM, Jett JR (1997) Superior pulmonary sulcus tumors and Pancoast's syndrome. N Engl J Med 337: 1370–1376
39. Ginsberg RJ (1995) Resection of a superior sulcus tumor. Chest Surg Clin North Am 5: 315–331
40. Dartevelle P, Macchiarini P (1999) Surgical management of superior sulcus tumors. Oncologist 4: 398–407
41. Dartevelle PG, Chapelier AR, Macchiarini P, Lenot B, Cerrina J, Ladurie FL, Parquin FJ, Lafont D (1993) Anterior transcervical-thoracic approach for radical resection of lung tumors invading the thoracic inlet. J Thorac Cardiovasc Surg 105: 1025–1034
42. Fadel E, Chapelier A, Bacha E, Leroy-Ladurie F, Cerrina J, Macchiarini P, Dartevelle P (1999) Subclavian artery resection and reconstruction for thoracic inlet cancers. J Vasc Surg 29: 581–588
43. Dartevelle PG (1997) Herbert Sloan Lecture. Extended operations for the treatment of lung cancer. Ann Thorac Surg 63: 12–19
44. York JE, Walsh GL, Lang FF, Putnam JB, McCutcheon IE, Swisher SG, Komaki R, Gokaslan ZL (1999) Combined chest wall resection with vertebrectomy and spinal reconstruction for the treatment of Pancoast tumors. J Neurosurg 91: 74–80
45. Heelan RT, Demas BE, Caravelli JF, Martini N, Bains MS, McCormack PM, Burt M, Panicek DM, Mitzner A (1989) Superior sulcus tumors: CT and MR imaging. Radiology 170: 637–641
46. McLoud TC, Filion RB, Edelman RR, Shepard JA (1989) MR imaging of superior sulcus carcinoma. J Comput Assist Tomogr 13: 233–239
47. Freundlich IM, Chasen MH, Varma DGK (1996) Magnetic resonance imaging of pulmonary apical tumors. J Thorac Imaging 11: 210–222
48. Haramati LB, White CS (2000) MR imaging of lung cancer. MRI Clin North Am 8: 43–57
49. Diaz-Arrastia R, Younger DS, Hair L, Inghirami G, Hays AP, Knowles DM, Odel JG, Fetell MR, Lovelace RE, Rowland LP (1992) Neurolymphomatosis: a clinicopathologic syndrome reemerges. Neurology 42: 1136–1141
50. Case records of the Massachusetts General Hospital (1995) Case 8–1995. N Engl J Med 332: 730–737
51. Swarnkar A, Fukui MB, Fink DJ, Rao GR (1997) MR imaging of brachial plexopathy in neurolymphomatosis. AJR 169: 1189–1190
52. Kori SH, Foley KM, Posner JB (1981) Brachial plexus lesions in patients with cancer: 100 cases. Neurology 31: 45–50
53. Kori SH (1995) Diagnosis and management of brachial plexus lesions in cancer patients. Oncology 9: 756–760
54. Bowen BC, Verma A, Brandon AH, Fiedler JA (1996) Radiation-induced brachial plexopathy: MR and clinical findings. AJNR 17: 1932–1936
55. Moore NR, Dixon AK, Wheeler TK, Freer CEL, Hall LD, Sims C (1990) Axillary fibrosis or recurrent tumour. An MRI study in breast cancer. Clin Radiol 42: 42–46
56. Thyagarajan D, Cascino T, Harms G (1995) Magnetic resonance imaging in brachial plexopathy of cancer. Neurology 45: 421–427
57. Iyer RB, Fenstermacher MJ, Libshitz HI (1996) MR imaging of the treated brachial plexus. AJR 167: 225–229
58. Van Es HW, Engelen AM, Witkamp TD, Ramos LMP, Feldberg MAM (1997) Radiation-induced brachial plexopathy: MR imaging. Skeletal Radiol 26: 284–288
59. Lingawi SS, Bilbey JH, Munk PL, Poon PY, Allan BM, Olivotto IA, Marchinkow LO (1999) MR imaging of brachial plexopathy in breast cancer patients without palpable recurrence. Skeletal Radiol 28: 318–323
60. Qayyum A, MacVicar AD, Padhani AR, Revell P, Husband JE (2000) Symptomatic brachial plexopathy following treatment for breast cancer: utility of MR imaging with surface-coil techniques. Radiology 214: 837–842
61. Ochi M, Ikuta Y, Watanabe M, Kimori K, Itoh K (1994) The diagnostic value of MRI in traumatic brachial plexus injury. J Hand Surg 19B:55–59
62. Walker AT, Chaloupka JC, Lotbiniere ACJ de, Wolfe SW, Goldman R, Kier EL (1996) Detection of nerve rootlet avulsion on CT myelography in patients with birth palsy and brachial plexus injury after trauma. AJR 167: 1283–1287
63. Gasparotti R, Ferraresi S, Pinelli L, Crispino M, Pavia M, Bonetti M, Garozzo D, Manara O, Chiesa A (1997) Three-dimensional MR myelography of traumatic injuries of the brachial plexus. AJNR 18: 1733–1742
64. Carvalho GA, Nikkhah G, Matthies C, Penkert G, Samii M (1997) Diagnosis of root avulsions in traumatic brachial plexus injuries: value of computerized tomography myelography and magnetic resonance imaging. J Neurosurg 86: 69–76
65. Mehta VS, Banerji AK, Tripathi RP (1993) Surgical treatment of brachial plexus injuries. Br J Neurosurg 7: 491–500
66. England JD, Tiel RL (1999) AAEM case report 33: costoclavicular mass syndrome. American Association of Electrodiagnostic Medicine. Muscle Nerve 22: 412–418
67. Berger A, Becker MHJ (1994) Brachial plexus surgery: our concept of the last twelve years. Microsurgery 15: 760–767
68. Wilbourn AJ, Porter JM (1988) Thoracic outlet syndromes: state of the art reviews. Spine 2: 597–626
69. Le Forestier N, Moulonguet A, Maisonobe T, Leger J-M, Bouche P (1998) True neurogenic thoracic outlet syndrome: electrophysiological diagnosis in six cases. Muscle Nerve 21: 1129–1134

70. Wilbourn AJ (1988) Thoracic outlet syndrome surgery causing severe brachial plexopathy. Muscle Nerve 11: 66–74
71. Hardy RWJ, Wilbourn AJ, Hanson M (1980) Surgical treatment of compressive cervical band. Neurosurgery 7: 10–13
72. Cherington M, Happer I, Machanic B, Parry L (1986) Surgery for thoracic outlet syndrome may be hazardous to your health. Muscle Nerve 9: 632–634
73. Wilbourn AJ (1990) The thoracic outlet syndrome is overdiagnosed. Arch Neurol 47: 328–330
74. Dymarkowski S, Bosmans H, Marchal G, Bogaert J (1999) Three-dimensional MR angiography in the evaluation of thoracic outlet syndrome. AJR 173: 1005–1008
75. Ohkawa Y, Isoda H, Hasegawa S, Furuya Y, Takahashi M, Kaneko M (1992) MR angiography of thoracic outlet syndrome. J Comput Assist Tomogr 16: 475–477
76. Panegyres PK, Moore N, Gibson R, Rushworth G, Donaghy M (1993) Thoracic outlet syndromes and magnetic resonance imaging. Brain 116: 823–841
77. Cherington M, Wilbourn AJ, Schils J, Whitaker J (1995) Thoracic outlet syndromes and MRI. Brain 118: 819–821
78. Subramony SH (1988) AAEE case report #14: neuralgic amyotrophy (acute brachial neuropathy). Muscle Nerve 11: 39–44
79. Tsairis P, Dyck PJ, Mulder DW (1972) Natural history of brachial plexus neuropathy. Report on 99 patients. Arch Neurol 27: 109–117
80. Suarez GA, Giannini C, Bosch EP, Barohn RJ, Wodak J, Ebeling P, Anderson R, McKeever PE, Bromberg MB, Dyck PJ (1996) Immune brachial plexus neuropathy: suggestive evidence for an inflammatory-immune pathogenesis. Neurology 46: 559–561
81. Bredella MA, Tirman PF, Fritz RC, Wischer TK, Stork A, Genant HK (1999) Denervation syndromes of the shoulder girdle: MR imaging with electrophysiologic correlation. Skeletal Radiol 28: 567–572
82. Helms CA, Martinez S, Speer KP (1998) Acute brachial neuritis (Parsonage-Turner syndrome): MR imaging appearance: report of three cases. Radiology 207: 255–259
83. Barohn RJ, Kissel JT, Warmolts JR, Mendell JR (1989) Chronic inflammatory demyelinating polyradiculoneuropathy. Clinical characteristics, course, and recommendations for diagnostic criteria. Arch Neurol 46: 878–884
84. Pestronk A, Cornblath DR, Ilyas AA, Baba H, Quarles RH, Griffin JW, Alderson K, Adams RN (1988) A treatable multifocal motor neuropathy with antibodies to GM1 ganglioside. Ann Neurol 24: 73–78
85. Ad Hoc Subcommittee of the American Academy of Neurology AIDS Task Force (1991) Research criteria for diagnosis of chronic inflammatory demyelinating polyneuropathy (CIDP). Neurology 41: 617–618
86. Duggins AJ, McLeod JG, Pollard JD, Davies L, Yang F, Thompson EO, Soper JR (1999) Spinal root and plexus hypertrophy in chronic inflammatory demyelinating polyneuropathy. Brain 122: 1383–1390
87. Van den Bergh PY, Thonnard JL, Duprez T, Laterre EC (2000) Chronic demyelinating hypertrophic brachial plexus neuropathy. Muscle Nerve 23: 283–288
88. Van Es HW, Van den Berg LH, Franssen H, Witkamp TD, Ramos LMP, Notermans NC, Feldberg MAM, Wokke JHJ (1997) Magnetic resonance imaging of the brachial plexus in patients with multifocal motor neuropathy. Neurology 48: 1218–1224